

0098

REPORT DOCUMENTATION

1a. REPORT SECURITY CLASSIFICATION <b>Unclassified</b>		1b. RESTRICTED	
2a. SECURITY CLASSIFICATION AUTHORITY		3. DISTRIBUTION STATEMENT A	
2b. DECLASSIFICATION/DOWNGRADING SCHEDULE		Approved for public release; Distribution unlimited.	
4. PERFORMING ORGANIZATION REPORT NUMBER(S)		5. MONITORING ORGANIZATION REPORT NUMBER(S)	
6a. NAME OF PERFORMING ORGANIZATION Department of Chemistry University of Denver	6b. OFFICE SYMBOL (If applicable) <b>NL</b>	7a. NAME OF MONITORING ORGANIZATION <b>SAME AS 8A</b>	
6c. ADDRESS (City, State and ZIP Code) Denver, Colorado 80208		7b. ADDRESS (City, State and ZIP Code) <b>SAME AS 8C</b>	
8a. NAME OF FUNDING/SPONSORING ORGANIZATION AFOSR/NL	8b. OFFICE SYMBOL (If applicable) <b>NL</b>	9. PROCUREMENT INSTRUMENT IDENTIFICATION NUMBER F49620-93-1-0631	
8c. ADDRESS (City, State and ZIP Code) 110 Duncan Avenue, Room B115 Bolling AFB, DC 20332-8080		10. SOURCE OF FUNDING NOS.	
11. TITLE (Include Security Classification) Physical Chemistry of Energetic Nitrogen Compounds		PROGRAM ELEMENT NO. <b>61102F</b>	PROJECT NO. <b>2303</b>
12. PERSONAL AUTHOR(S) Robert D. Coombe		TASK NO. <b>ES</b>	WORK UNIT NO.
13a. TYPE OF REPORT Final Report	13b. TIME COVERED FROM <b>01-Nov-93</b> TO <b>31-Nov-96</b>	14. DATE OF REPORT (Yr., Mo., Day) 01-Feb-97	15. PAGE COUNT
16. SUPPLEMENTARY NOTATION			
17. COSATI CODES		18. SUBJECT TERMS (Continue on reverse if necessary and identify by block number)	
FIELD	GROUP	SUB. GR.	
		azides, amines, nitrenes, aminyl radicals, azide radicals, reactions, lasers, energy transfer, excited states, thin films, nitrides, boron azides, aluminum azides, gallium azides	
19. ABSTRACT (Continue on reverse if necessary and identify by block number)			
<p>This three year research program was comprised of several projects grouped into three areas, which were the chemistry of <math>CIN_3</math> dissociation and the <math>NCl/I^*</math> laser system, <math>NH(a^1\Delta)</math> insertion reactions with molecular halogens and interhalogens, and the synthesis and characterization of group III azides and their decomposition to form group III nitride thin films. The results obtained included the demonstration of a new chemical laser (NILE, or nitrene-iodine-laser-experiment) based on energy transfer from <math>NCl(a^1\Delta)</math> to iodine atoms, enhanced understanding of the dynamics of an entire group of reactions with halogen amine intermediates, the first spectroscopic characterizations of fully azide substituted boron, aluminum, and gallium compounds, and the demonstration of low temperature methods for the deposition of BN and AlN thin films.</p>			
20. DISTRIBUTION/AVAILABILITY OF ABSTRACT UNCLASSIFIED/UNLIMITED <input checked="" type="checkbox"/> SAME AS RPT. <input type="checkbox"/> DTIC USERS <input type="checkbox"/>		21. ABSTRACT SECURITY CLASSIFICATION Unclassified	
22a. NAME OF RESPONSIBLE INDIVIDUAL Robert D. Coombe / <b>Michael R. Berman</b>		22b. TELEPHONE NUMBER (Include Area Code) <b>(303)-871-2693</b> <b>202-762-9963</b>	22c. OFFICE SYMBOL <b>NL</b>

## CONTENTS

<b>Introduction</b>	1
<b>The <math>\text{ClN}_3</math> Chain and the NILE Laser Device</b>	2
1. Quenching of $\text{NCl}(a^1\Delta)$ and the Chain Decomposition of $\text{ClN}_3$	2
2. Demonstration of an $\text{I}^*$ Laser Pumped by $\text{NCl}(a^1\Delta)$	2
3. Chemical Production of Excited Nitrenes and Energy Transfer to Iodine	8
<b><math>\text{NH}(a^1\Delta)</math> Insertion Reactions</b>	10
<b>Synthesis of Group III Azides and Deposition of III-V Thin Films</b>	12
1. Gas Phase Synthesis, Structure, and Decomposition of Boron Triazide	12
2. Aluminum Azides and AlN Thin Films	16
3. The Reaction of $\text{Ga}(\text{CH}_3)_3$ with $\text{HN}_3$	22
<b>Conclusions and Future Work</b>	23
<b>Publications Arising From This Work</b>	24
<b>Personnel</b>	25
<b>References</b>	25

19970227 061

## INTRODUCTION

This report describes the results of research performed during the period 1 November, 1993 through 31 November, 1996 under the auspices of AFOSR grant number F49620-93-1-0631. The program, "Physical Chemistry of Energetic Nitrogen Compounds", had as its global objective the development of a better understanding of the mechanisms of energy storage in highly energetic or metastable molecules, and of the processes which occur when such molecules are stimulated by photolysis, reaction, or collisional energy transfer. This program represents the last three year period of a long term research effort spanning several years. Much of the work done over this longer period has involved study of energetic nitrogen - bearing molecules such as azides, isocyanates, amines, and related radical species such as nitrenes and aminyls.

The program was comprised of a number of projects included within three broader research areas, which were aspects of the NCI/I\* laser device, the dynamics of  $\text{NH}(a^1\Delta)$  insertion reactions, and the synthesis of group III azides and their decomposition to form III-V thin films. Data obtained from the individual research projects are relevant to a number of application of interest to the Air Force, in particular lasers, energetic materials, and electronic materials.

The NCI/I\* laser device, dubbed the "NILE" for Nitrene-Iodine-Laser-Experiment, was discovered in our laboratory as part of this AFOSR program. The laser demonstration, accomplished in 1994 and published in 1995, was based on excitation of iodine atoms in collisions with electronically excited  $\text{NCI}(a^1\Delta)$ . The excited NCI was obtained from the chain decomposition of  $\text{CIN}_3$  initiated by UV photolysis. A related project was also completed which probed the mechanism of the  $\text{CIN}_3$  chain and the rates of quenching of excited NCI by species present in the reaction mixture. The success of the laser demonstration stimulated the initiation of a research effort at the Air Force Phillips Laboratory at Kirtland AFB (New Mexico) directed toward the demonstration of a cw device for which  $\text{NCI}(a^1\Delta)$  is generated by the  $\text{Cl} + \text{N}_3$  reaction. Researchers at the Phillips Lab also began investigations of the kinetics of second-order processes potentially important to the operation of the laser at high reagent densities. Another project was performed in our laboratory to support these efforts at the Phillips Lab. This project was based on lower density discharge-flow experiments, and sought to determine the efficiency of the  $\text{Cl} + \text{N}_3$  reaction as a source of excited NCI, and also whether iodine atoms might be excited by  $\text{NF}(a^1\Delta)$ , a possibility which would open up attractive alternatives for pumping the cw laser device.

The second program area involved studies of the dynamics of  $\text{NH}(a^1\Delta)$  insertion reactions. This work was based on the hypothesis that such insertions would produce amine-like intermediate molecules similar to a number of halogenated amines studied previously in our lab. Analysis of the products of the insertion reactions and comparison with those produced from dissociation of the halogen amines offered insights into the mechanisms of both systems. Interestingly, our work in this area also led to a current research program in our laboratory, which is directed toward exploring  $\text{NH}(a^1\Delta)$  insertion processes useful for the generation of GaN thin films.

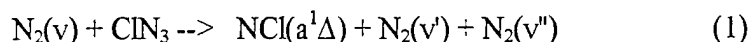
The third research area involved the synthesis of novel group III azides and exploration of their utility for the low temperature deposition of III-V thin films. This work began serendipitously, in the course of our study on  $\text{NH}(a^1\Delta)$  insertion into  $\text{BCl}_3$ . As it happened, the precursor of the excited  $\text{NH}$ ,  $\text{HN}_3$ , undergoes a spontaneous room temperature reaction with  $\text{BCl}_3$  in which the Cl atoms are replaced by  $\text{N}_3$  leading to a fully azidified boron compound  $\text{B}(\text{N}_3)_3$ . This is a highly energetic species which decays to BN films and  $\text{N}_2$ . Subsequent work in our lab led to the generation of azides of aluminum and gallium, and the deposition of AlN and GaN films. These materials are important for a number of applications in optics and optoelectronics.

A number of individual projects were performed within each of these three areas. Since the results of these projects have in large measure been described in the open literature, we present below only a brief summary of each project, along with an assessment of the significance of the results.

## THE $\text{ClN}_3$ CHAIN AND THE NILE LASER DEVICE

### 1. Quenching of $\text{NCl}(a^1\Delta)$ and the Chain Decomposition of $\text{ClN}_3$

This task was begun during a previous funding period (grant number AFOSR-90-0259) and was completed during the first year of the current program. It was also supported in part by another AFOSR program, grant number F49620-J-0270. This work explored the chain decomposition of  $\text{ClN}_3$  initiated by photolysis of this compound at 193 nm and 249 nm. The initial photolytic event produces  $\text{NCl}(a^1\Delta)$  and  $\text{N}_2$ , with the nitrogen molecule expected to have considerable vibrational excitation<sup>1</sup>. The vibrationally excited  $\text{N}_2$  can then carry the chain decomposition of the  $\text{ClN}_3$  as follows:



Both  $\text{NCl}(a^1\Delta)$  and vibrationally excited  $\text{N}_2$  are regenerated by this collisional dissociation of the fragile  $\text{ClN}_3$ , a molecule in which  $\text{NCl}(a^1\Delta)$  and  $\text{N}_2$  are bound<sup>2</sup> by only about 16 kcal/mole. Following this model, it is expected that the observed time decay of 1.08  $\mu\text{m}$  emission from  $\text{NCl}(a^1\Delta)$  produced by the photolysis tracks the overall loss of  $\text{ClN}_3$  from the system.

The chain can be avoided when the  $\text{ClN}_3$  density is low, such that the  $\text{NCl}(a^1\Delta) - \text{ClN}_3$  collision time is long relative to diffusion to the vessel walls. In this case the emission from  $\text{NCl}(a^1\Delta)$  is observed to decay exponentially, with a decay time which varies inversely with the density of added quenchers, and is limited by the diffusion rate, which is controlled by the density of the rare gas diluent. These conditions were employed to measure rate constants for  $\text{NCl}(a^1\Delta, v=0)$  quenching by collisions with added gases. Rate constants were measured for quenching by  $\text{H}_2$ ,  $\text{D}_2$ ,  $\text{HCl}$ ,  $\text{DCl}$ ,  $\text{HF}$ ,  $\text{O}_2$ ,  $\text{Cl}_2$ ,  $\text{He}$ , and  $\text{Ar}$ . These parameters are important in modeling the performance of several methods for the chemical generation of  $\text{NCl}(a^1\Delta)$ , in particular the reactions of chloroamines with hydrogen or deuterium atoms. These systems are of interest with respect to the development of  $\text{NCl}(a^1\Delta)/\text{I}^*$  lasers.

A paper describing these the details of these experiments was published<sup>3</sup> in the Journal of Physical Chemistry in August of 1994.

## 2. Demonstration of an I\* Laser Pumped by NCl(a<sup>1</sup>Δ)

In our previous AFOSR sponsored program, we did a thorough investigation<sup>4</sup> of the energy transfer process between excited NCl(a<sup>1</sup>Δ) and iodine atoms reported in 1991 by Bower and Yang.<sup>5</sup> Our experiment was based on the pulsed photolysis of mixtures of CIN<sub>3</sub> with CH<sub>2</sub>I<sub>2</sub> at 193 nm. At this wavelength, the CIN<sub>3</sub> is dissociated to produce NCl(a<sup>1</sup>Δ) and the CH<sub>2</sub>I<sub>2</sub> is dissociated to produce CH<sub>2</sub>I and iodine atoms, with a 5% branching fraction to I\*(5<sup>2</sup>P<sub>1/2</sub>). The presence of the CIN<sub>3</sub> was found to enhance the intensity of 1.315 μm emission from the I\* by up to a factor of 5, and the rate constant for the energy transfer process was determined<sup>4</sup> from a steady state analysis of the data. From the time profile of the I\* emission, it was clear that the iodine atoms were not rapidly lost from the system, but were cycled between the 5<sup>2</sup>P<sub>3/2</sub> and 5<sup>2</sup>P<sub>1/2</sub> states many times during the several millisecond period of the emission. This information was correlated with the chain decomposition of CIN<sub>3</sub>, which was subsequently studied in the project described above.

It was evident from these data that the CIN<sub>3</sub>/CH<sub>2</sub>I<sub>2</sub> system might well be driven to produce a population inversion among the iodine atoms (which requires that 1/3 of the atoms be in the 5<sup>2</sup>P<sub>1/2</sub> state), and perhaps even to a lasing condition if a sufficient inversion density were to be created. To test this possibility, an apparatus like that shown in Figure 1 was constructed. The design incorporates a longitudinally pumped reaction cell, with an

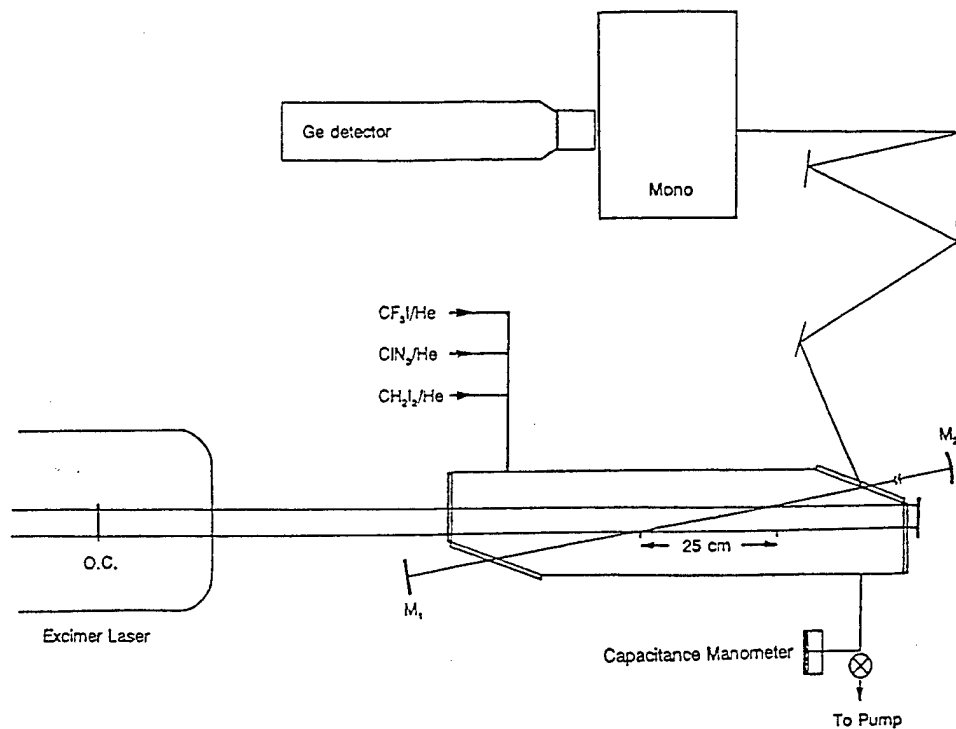


Figure 1. Apparatus for pulsed NCl/I\* laser demonstration.

off-axis optical cavity producing a 25 cm gain length. The cavity end mirrors were dielectrics coated for maximum reflectivity at 1.315  $\mu\text{m}$ , and were arranged for a folded near-confocal cavity. The threshold inversion density (defined as  $[I^*] - (1/2)[I]$ ) for lasing in this cavity was determined by photolysis of  $\text{CF}_3\text{I}/\text{He}$  mixtures<sup>6</sup> at 249 nm, for measured laser fluences. The threshold inversion density was found to be about  $1.1 \times 10^{14} \text{ cm}^{-3}$ .

Chlorine azide gas was produced<sup>1</sup> in a continuous flow by passage of a dilute mixture of  $\text{Cl}_2$  in He over moistened  $\text{NaN}_3$  suspended on glass wool at 273K. Its density in the effluent of the reactor was monitored continuously by calibrated infrared absorption.  $\text{CH}_2\text{I}_2$  was purified by freeze-thaw cycles and the vapor mixed with He and stored in a pyrex bulb. The  $\text{ClN}_3$  and  $\text{CH}_2\text{I}_2$  flowed continuously through the cell shown in Figure 1, at flow rates such that the density of  $\text{CH}_2\text{I}_2$  was near  $2 \times 10^{14} \text{ cm}^{-3}$  and the density of  $\text{ClN}_3$  was on the order of  $5 \times 10^{15} \text{ cm}^{-3}$ .

A mirror coated for maximum reflectivity at 193 nm was positioned at the exit end of the cell as shown in the Figure, to reflect excimer laser radiation transmitted by the cell back through the medium. This arrangement is very nearly that of an intracavity absorption experiment, with most of the radiation losses occurring at the output coupler of the laser and the windows of the cell. When laser radiation scattered from the cell windows was monitored, it was observed that virtually all of this radiation was extinguished when the  $\text{ClN}_3/\text{CH}_2\text{I}_2$  mixture was present in the cell, suggesting that light not lost at the output coupler or windows is absorbed by the gases. From this information, we estimate the initial density of  $\text{NCl}(a^1\Delta)$  to be near  $2.5 \times 10^{15} \text{ cm}^{-3}$ . Because of its very large absorption cross section,<sup>7</sup> essentially all of the  $\text{CH}_2\text{I}_2$  present is dissociated to  $\text{CH}_2\text{I}$  and iodine atoms. Based on a simple steady state analysis<sup>14</sup> in which the rate of  $I^*$  pumping by  $\text{NCl}(a^1\Delta)$  is balanced with the rate of its quenching in collisions with residual  $\text{ClN}_3$ , these densities are such that the inversion density in the system should be within a factor of 2 of laser threshold, i.e., within the global uncertainty of our knowledge of the rate constants of the processes involved.

Figure 2a shows the time profile of  $I^*$  emission observed for an experiment in which the inversion density was near but sub-threshold. The emission persists over several milliseconds, and shows several clear "ripples" in the vicinity of the intensity maximum. These ripples were also observed in the time profiles of  $I^*$  emission from  $\text{CF}_3\text{I}$  photolysis under just sub-threshold conditions. Figure 2b shows a case in which the system has indeed reached threshold, as indicated by the fact that one of the ripples has become an intense spike, occurring 400  $\mu\text{s}$  after the 193 nm photolysis. For this condition, threshold was still reached on the next photolysis pulse (after the cell was given time to purge the gas mixture), but the laser pulse was much less intense and the threshold time was near 2 ms. Figure 2c shows a laser pulse obtained with different reagent densities. In this case, the  $\text{ClN}_3$  density was much higher and the  $\text{CH}_2\text{I}_2$  density was much smaller than for the data in Figure 2b. The simple steady state consideration suggests that threshold should not be reached for these conditions, yet it clearly is. Further, the threshold time is quite long, at nearly 2 ms after the photolysis laser pulse. Here again, the laser reached threshold again on the very next laser pulse, but with diminished intensity and a still longer threshold time. Clearly, the situation is more complex than that described by the steady state model (in which the laser threshold is established by the photolysis pulse, and lasing would occur within 50  $\mu\text{s}$  after photolysis). We note here that laser pulses such as those

shown in Figure 2 were obtained in many different experiments, and that lasing was not observed unless both  $\text{ClN}_3$  and  $\text{CH}_2\text{I}_2$  were present, and unless the cavity the optical cavity was very well aligned and the gases at their highest purities. The system was very clearly near threshold, and indeed the laser did not operate on every photolysis pulse even with the best of conditions as limited by the capabilities of our apparatus.

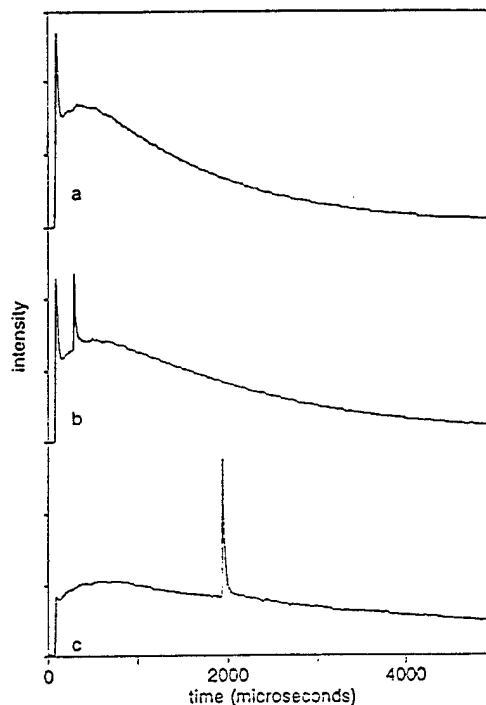


Figure 2. (a) Time profile of  $\text{I}^*$  chemiluminescence at  $1.315 \mu\text{m}$ , produced by photolysis of  $2.8 \times 10^{14} \text{ cm}^{-3} \text{ CH}_2\text{I}_2$  and  $4.5 \times 10^{15} \text{ cm}^{-3} \text{ ClN}_3$  at 193 nm. (b)  $\text{I}^*$  emission time profile, with lasing event, produced by photolysis of  $2.8 \times 10^{14} \text{ cm}^{-3} \text{ CH}_2\text{I}_2$  and  $4.5 \times 10^{15} \text{ cm}^{-3} \text{ ClN}_3$  at 193 nm. (c)  $\text{I}^*$  emission time profile, with lasing event, produced by photolysis of  $1.5 \times 10^{14} \text{ cm}^{-3} \text{ CH}_2\text{I}_2$  and  $8.9 \times 10^{15} \text{ cm}^{-3} \text{ ClN}_3$  at 193 nm.

From the long threshold times, it seems apparent that the chemistry occurring after the photolysis pulse somehow serves to help create the inversion density, in the manner of a true chemical laser. To further investigate this issue, we assembled a kinetic model for the system based upon our knowledge of the  $\text{NCl}(a^1\Delta) - \text{I}$  energy transfer process and the photochemistry and chain decomposition of  $\text{ClN}_3$ . The processes included in the model and their rate constants are shown in Table I. Note that in the model the chain decomposition of  $\text{ClN}_3$  is carried by both  $\text{I}^*$  and vibrationally excited  $\text{N}_2$ , consistent with the conclusions of our earlier work on this subject. We have also included  $\text{I}^*$  quenching by  $\text{CH}_2\text{I}$  and  $\text{I}_2$ , as well as first order losses of  $\text{I}^*$ ,  $\text{I}$ , and  $\text{NCl}(a)$  by diffusion. The amount of  $\text{I}_2$  initially present (corresponding to about a 3% yield from the photolysis of  $\text{CH}_2\text{I}_2$ ) was chosen to give good agreement with the observed  $\text{I}^*$  time decay. Another important feature is the inclusion of second order loss of  $\text{NCl}(a^1\Delta)$  by self annihilation. The rate constant chosen for this process,  $8.0 \times 10^{-12} \text{ cm}^3$ , is that reported by Benard and co-workers.<sup>2</sup> Inclusion of this process at this rate gives good agreement with the observed time decay of the  $\text{NCl}(a^1\Delta)$  density in our system.

Figure 3 shows the results obtained from numerical integration of the differential rate equations corresponding to the kinetic model, for for initial conditions of the experimental result shown in Figure 2b. The agreement with the experimental  $I^*$  time profile is excellent (as is the agreement with the  $\text{NCl}(a^1\Delta)$  time profile). It is clear from these results that the laser reaches threshold when the chain has removed the  $\text{CIN}_3$  from the system. At this point, the density of  $\text{NCl}(a^1\Delta)$  remaining is sufficient to almost completely invert the iodine atoms present. The  $I^*$  thus produced is not quenched by the

Table I. Kinetic Model for the NILE

Reaction	$k(\text{cm}^3 \text{ molecule}^{-1} \text{ s}^{-1})$
$\text{NCl}(a) + \text{I} \rightarrow \text{I}^* + \text{NCl}(X)$	$1.8 \times 10^{-11}$
$\text{I}^* + \text{CIN}_3 \rightarrow \text{I} + \text{NCl}(a) + \text{N}_2(v)$	$2.0 \times 10^{-11}$
$\text{NCl}(a) + \text{CIN}_3 \rightarrow \text{NCl}(x) + \text{NCl}(a) + \text{N}_2$	$2.0 \times 10^{-11}$
$\text{N}_2(v) + \text{CIN}_3 \rightarrow \text{NCl}(a) + \text{N}_2 + \text{N}_2$	$1.0 \times 10^{-11}$
$\text{NCl}(a) + \text{NCl}(a) \rightarrow 2 \text{Cl} + \text{N}_2(v)$	$8.0 \times 10^{-12}$
$\text{I}^* + \text{CH}_2\text{I} \rightarrow \text{I} + \text{CH}_2\text{I}$	$4.0 \times 10^{-13}$
$\text{I}^* + \text{I}_2 \rightarrow \text{I} + \text{I}_2$	$3.6 \times 10^{-11}$
$\text{I}^* \rightarrow \text{loss by diffusion}$	$360 \text{ s}^{-1}$
$\text{I} \rightarrow \text{loss by diffusion}$	$360 \text{ s}^{-1}$
$\text{NCl}(a) \rightarrow \text{loss by diffusion}$	$480 \text{ s}^{-1}$

ground state  $\text{NCl}$  (also present in substantial density) since this must be a non-resonant E to V,R or E to T process and hence should be slow. The  $I^*$  population generated as the  $\text{CIN}_3$  decays is lost by the quenching mechanism noted above, which assumes the production of ground state iodine atoms (in fact, we do not know that this is the case). Assuming a threshold inversion density of about  $1 \times 10^{14} \text{ cm}^{-3}$  as discussed above, the laser should reach threshold at about  $200 \mu\text{s}$ . This value is shorter by about a factor of two than the observed threshold, but the result is still in substantial agreement with the data.

Figure 4 shows the result of the model calculation for the conditions of the data in Figure 2c. The calculated time profile of the  $I^*$  emission is again in excellent agreement with the data. In this case, the chain decomposition of the  $\text{CIN}_3$  is extended in time because the starting density of the azide is higher and, because the initial density of  $\text{CH}_2\text{I}_2$  is lower, the density of  $I^*$  chain carriers is lower. The laser again reaches threshold when the  $\text{CIN}_3$  is gone, in this case with a threshold time of about  $800 \mu\text{s}$ . This result is certainly in qualitative accord with the data, since it shows that the system should still lase in spite of the large initial  $\text{CIN}_3$  density, and that the threshold time is considerably extended relative to the conditions of Figure 2b.

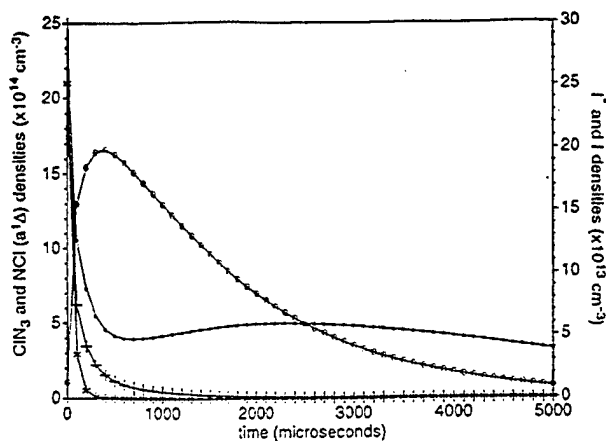


Figure 3 Results of the kinetic model for the reagent densities in Figure 2b. Legend:  $\circ = \text{I}^*$ ,  $\bullet = \text{I}$ ,  $+$  =  $\text{NCl}^*$ , and  $\star = \text{CIN}_3$ .

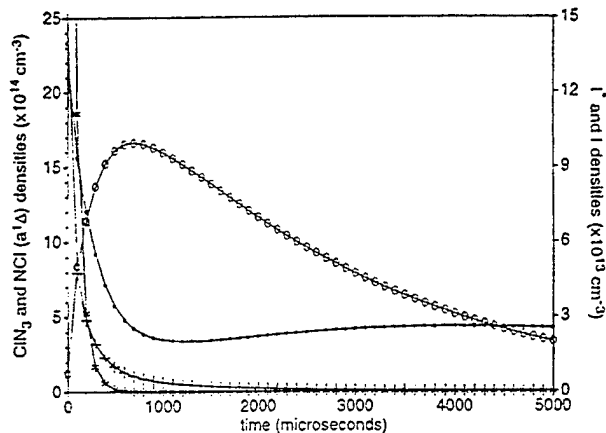


Figure 4 Results of the kinetic model for the reagent densities in Figure 2c. Legend:  $\circ = \text{I}^*$ ,  $\bullet = \text{I}$ ,  $+$  =  $\text{NCl}^*$ , and  $\star = \text{CIN}_3$ .

For both the smaller and larger  $\text{CIN}_3$  densities (Figures 2b and 2c), the laser reaches threshold later than the model predicts it should. Further, in both cases the next laser pulse still reached threshold, but was delayed in time still further. Calculations with the model have indicated that this behavior is not a function of collisional quenching of  $\text{I}^*$ ; such quenching would reduce the gain but would not extend the threshold time, which is set by the loss of  $\text{CIN}_3$  from the system. Artificially extending the  $\text{CIN}_3$  loss by reducing the rates in the chain or by allowing for quenching of  $\text{N}_2(v)$ , for example, certainly lengthens the threshold time but the  $\text{I}$  and  $\text{NCl}(a)$  time profiles no longer match the experimental data. At this point, we believe that the extended thresholds may be caused by the presence of a transient  $1.3 \mu\text{m}$  absorber. Such an absorber would be produced by the UV photolysis pulse, and would be removed from the gain region by diffusion. Indeed, our calculations have shown that the time regime of diffusion in the system is in fact just right for producing such an effect. There are two possibilities for such an absorber. The first of these is  $\text{CH}_2\text{I}$  radicals. These radicals might absorb at  $1.3 \mu\text{m}$  via overtones of the C-H stretching vibrations. Since the laser is very near threshold, only a tiny absorption in the gain region would be sufficient to lengthen the threshold time. The

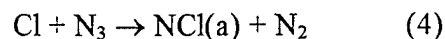
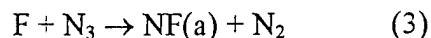
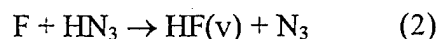
second and more likely possibility is I<sub>2</sub>. This species is surely present in gas mixture since we see its characteristic violet luminescence on photolysis at 193 nm. Vacuum UV photolysis of CH<sub>2</sub>I<sub>2</sub> is known<sup>8</sup> to produce I<sub>2</sub>, and it is certainly possible that a small amount is produced by photolysis at 193 nm. This was included in the model as noted above. I<sub>2</sub> absorbs at wavelengths as long as 935 nm even at room temperature,<sup>9</sup> and moderate vibrational excitation (such as might easily be produced by photodissociation of CH<sub>2</sub>I<sub>2</sub>) would surely lead to absorption well beyond 1.3 μm. Further, I<sub>2</sub> is difficult to remove from the system by pumping, and could easily account for the extended threshold times on the "second" laser shots as described above. Clearly, more work is needed to clarify this issue and other details of the kinetics and optics of the system. We are currently addressing these issues in our laboratory.

Our work on the NILE laser demonstration was published<sup>10</sup> in the Journal of Physical Chemistry in March of 1995.

### 3. Chemical Production of Excited Nitrenes and Energy Transfer to Iodine

During the second year of the program, we began a project directed toward measurement of key parameters in the chemical generation of NCl(a) by the reaction of HN<sub>3</sub> with a mixture of F and Cl atoms, and the excitation of I\* by energy transfer from the excited NCl in this chemical medium. These measurements are important since Dr. Gordon Hager and co-workers at the Air Force Phillips Laboratory have selected this chemical system for demonstration of a cw NCl/I\* device. In particular, our study was directed toward better defining the NCl(a)/NCl(X) branching fraction produced by the Cl + N<sub>3</sub> reaction, the effects of adding various iodine sources to the reaction medium, and the possibility that I\* might be pumped directly by the NF(a) product of the F + N<sub>3</sub> reaction. Preliminary results were obtained during the second year of the program. This past year, experiments were completed in the Fall and modeling continued until recently. The modeling effort turned out to be a very significant task, particularly modeling of the system after different halogen sources (Cl<sub>2</sub> or DCl, I<sub>2</sub> or HI) were factored in.

The results of the branching study experiments are quite firm. In the experiments, NF(a) and NCl(a) are created by the following sequence of reactions:



Hence the mix of NCl(a) and NF(a) is controllable according to the amounts of F and Cl atoms present and the known rate constants of the three reactions shown. By measuring the intensities of emissions from NCl(a) and NF(a), corrected for the system response and published radiative rates<sup>11,12</sup>, and incorporating the data into a kinetic model for the system which includes all known pumping and quenching processes, the branching fraction to NCl(a) in the Cl + N<sub>3</sub> reaction can be obtained by using the known<sup>13</sup> branching fraction in the F + N<sub>3</sub> reaction as a standard. Alternatively, the branching fraction in Cl + N<sub>3</sub> can be

assumed to be equivalent to that in  $F + N_3$  and data used to calculate the radiative rate for the  $a \rightarrow X$  transition in  $NCl$ , for comparison with the rate calculated by Yarkony.<sup>11</sup>

Figure 5 shows experimental data and the results of calculations for the time profiles of  $NCl(a)$  and  $NF(a)$  in the reaction medium. For times beyond about 1.5 ms, the agreement is quite good. For shorter times, the  $NF(a)$  data includes a significant contribution from emission from  $HF$  on the  $v=3 \rightarrow v=0$  transition (in fact, modeling of the sum of the  $HF(v)$  and  $NF(a)$  emissions gives a time profile much like that shown in Figure 5). From data such as that shown in the Figure, and the assumption the branching fractions in  $Cl + N_3$  and  $F + N_3$  are equivalent at 0.9, we calculate an  $NCl(a)$  radiative rate  $\tau = 0.51 \text{ sec}^{-1}$ , in excellent agreement with Yarkony's calculated<sup>11</sup> rate,  $0.5 \text{ sec}^{-1}$ . We conclude that the branching fraction in  $Cl + N_3$  is indeed quite high, a result which certainly bodes well for the laser demonstration project at the Phillips Laboratory.

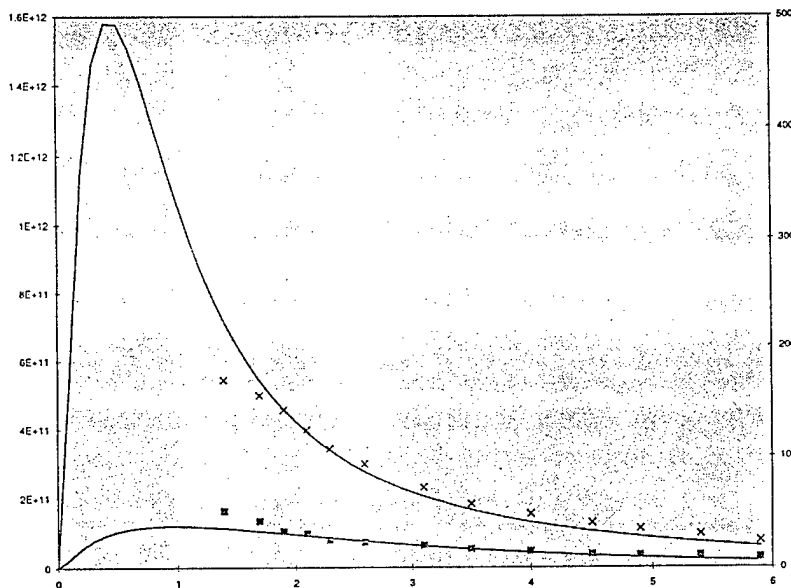


Figure 5. Experimental (solid lines) and calculated time profiles of  $NCl(a)$  and  $NF(a)$  produced by the  $F/Cl + HN_3$  reaction. Squares,  $NF(a)$ , crosses,  $NCl(a)$ .

The results regarding pumping of  $I^*$  by  $NF(a)$  are much less precise, largely because of a number of rather uncertain rate constants which must be included in the model. A number of these uncertain rates are associated with the reactions of  $I_2$  with halogen atoms ( $F$  and  $Cl$ ), to produce diatomic interhalogens which can quench various species in the reaction mixture. Although we cannot determine a precise branching fraction to  $I^*$  from  $NF(a)$  quenching by iodine atoms, we can set an upper limit. This process has a branching fraction which is surely less than 0.02 under the conditions of our experiments (small densities at room temperature). This result indicates that this process is *not* useful for pumping an  $I^*$  laser. Recently Benard<sup>14</sup> reported data which suggested that the branching fraction to  $I^*$  is much higher in a chemical system based on dissociation of  $FN_3$  in a shock tube. The discrepancy may be a result of the very different temperatures in the two cases,

although this seems unlikely. Our data suggest that the NCl(a)/I\* system is unique, and that the high branching fraction to I\* in this case is probably tied to nuances of the ClNI excited state potential energy surface over which the energy transfer process proceeds.

At the present time, we are preparing a manuscript which describes our experimental data and modeling of the Cl/F + HN<sub>3</sub> + I<sub>2</sub> system.

### NH(a<sup>1</sup>Δ) INSERTION REACTIONS

Previous work in our laboratory<sup>15</sup> has shown that the reaction of H atoms with NCl<sub>2</sub> radicals produces a high yield of NCl(a<sup>1</sup>Δ), presumably by the formation of a singlet dichloramine intermediate which eliminates HCl and the excited singlet NCl. The singlet potential energy surface of this reaction also correlates adiabatically to Cl<sub>2</sub> and excited NH(a<sup>1</sup>Δ), but these products are energetically inaccessible. This reasoning led to our speculation that the reverse, exothermic reaction between NH(a<sup>1</sup>Δ) and Cl<sub>2</sub> might well proceed by an insertion-elimination process in which a dichloramine intermediate is formed by NH(a<sup>1</sup>Δ) insertion, followed by spin constrained elimination to HCl and NCl(a<sup>1</sup>Δ). A preliminary investigation of this process indicated that this was indeed the case; photolysis of HN<sub>3</sub>/Cl<sub>2</sub> mixtures at either 193 nm or 249 nm (to produce NH(a<sup>1</sup>Δ)) was observed to lead to the generation of NCl(a<sup>1</sup>Δ) and vibrationally excited HCl. These preliminary results were published<sup>16</sup> in Chemical Physics Letters in late 1993.

As part of this AFOSR program, these results were extended to reactions between NH(a<sup>1</sup>Δ) and a variety of halogen and interhalogen molecules. The first part of this investigation involved measurements of rate constants of the overall quenching of NH(a<sup>1</sup>Δ, v=0) by collisions with these species. This was done by using time resolved laser-induced fluorescence on the NH a<sup>1</sup>Δ - c<sup>1</sup>Π transition near 325 nm to monitor the time decay of the NH(a<sup>1</sup>Δ) density after the 193 nm photolysis pulse. Typical data for quenching by ClF are shown in Figure 6, and all of the rate constants measured are gathered together in Table II. The data show an interesting trend. The largest rate constant was found for quenching by ICl. Quenching by Br<sub>2</sub> or Cl<sub>2</sub> is about a factor of two slower than quenching by ICl. Quenching by ClF is about a factor of four slower than quenching by ICl, and quenching by F<sub>2</sub> is very slow, if it happens at all. We believe that this trend has to do with the lability of the electrons in the bond between the halogen atoms. In the insertion process, these electrons are donated into an unoccupied non-bonding orbital (the LUMO) on the nitrogen atom of the NH(a<sup>1</sup>Δ) molecule. Since the bonding electrons in ICl are expected to be much more labile than those in F<sub>2</sub>, the rate of the insertion reaction is expected to be much faster with ICl.

Table II also shows the observed chemiluminescent products of the quenching reactions. For NH(a<sup>1</sup>Δ) quenching by Cl<sub>2</sub> and Br<sub>2</sub>, both the a<sup>1</sup>Δ and b<sup>1</sup>Σ<sup>+</sup> states of NCl and NBr, respectively, are found, along with IR emissions from the vibrationally excited hydrogen halide co-products. For NH(a<sup>1</sup>Δ) quenching by ClF, there are two possible product channels:

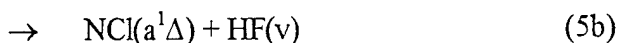
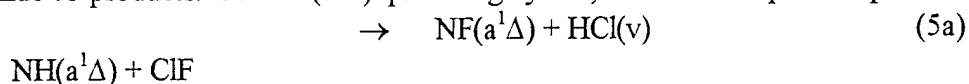


Table II.  $\text{NH}(a^1\Delta) + \text{XY}$  Reactions

XY	$k(\text{cm}^3 \text{ molecule}^{-1} \text{ s}^{-1})$	Products
$\text{F}_2$	$1.2 \times 10^{-13}$	
$\text{ClF}$	$3.5 \times 10^{-11}$	$\text{NCl}(a^1\Delta)$ , 5% $\text{NF}(a^1\Delta)$ , 95%
$\text{Cl}_2$	$7.5 \times 10^{-11}$	$\text{NCl}(a^1\Delta, b^1\Sigma^+)$ $\text{HCl}(v)$
$\text{Br}_2$	$6.0 \times 10^{-11}$	$\text{NBr}(a^1\Delta, b^1\Sigma^+)$ $\text{HBr}(v)$
$\text{ICl}$	$1.5 \times 10^{-10}$	

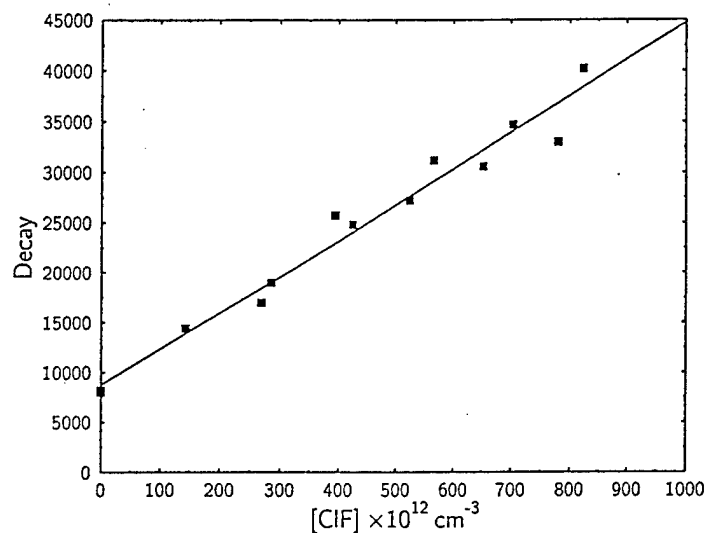


Figure 6.  $\text{NH}(a)$  quenching rate vs.  $\text{ClF}$  density.

In principle, this reaction may proceed via a singlet  $\text{HNFCI}$  intermediate analogous to that for the  $\text{H} + \text{NFCI}$  reaction, a process studied previously in our laboratory.<sup>17</sup> In these previous experiments (done with a continuous discharge-flow apparatus), the  $\text{H} + \text{NFCI}$  reaction was found to produce excited  $\text{NF}(a^1\Delta)$  in a ten-fold excess over  $\text{NCl}(a^1\Delta)$ . This result was verified in later experiments by Setser and co-workers.<sup>18</sup> If an analogous intermediate is indeed involved in reaction (5) above, the a similar preference for  $\text{NF}(a^1\Delta)$  formation would be expected. In the  $\text{NH}(a^1\Delta) + \text{ClF}$  experiment, both  $\text{NF}(a^1\Delta)$  and  $\text{NCl}(a^1\Delta)$  were indeed

observed, and the time profiles of emission from these species are shown in Figure 7. When these data are deconvoluted for the known radiative rates<sup>11,12</sup> of  $\text{NF}(a^1\Delta)$  and  $\text{NCl}(a^1\Delta)$  and the relative response of the filters and Ge detector used in the experiment, the density of  $\text{NF}(a^1\Delta)$  is found to be a factor of nearly 18 greater than that of  $\text{NCl}(a^1\Delta)$ . This result would surely seem to support our thoughts concerning the similarity of the intermediates of the  $\text{H} + \text{NFCl}$  and  $\text{NH}(a^1\Delta) + \text{ClF}$  reactions. At present, we are using computational methods to explore the characteristics of the potential energy surfaces of these most interesting reactions. A manuscript describing our experimental results was published in the *Journal of Physical Chemistry* in 1995.

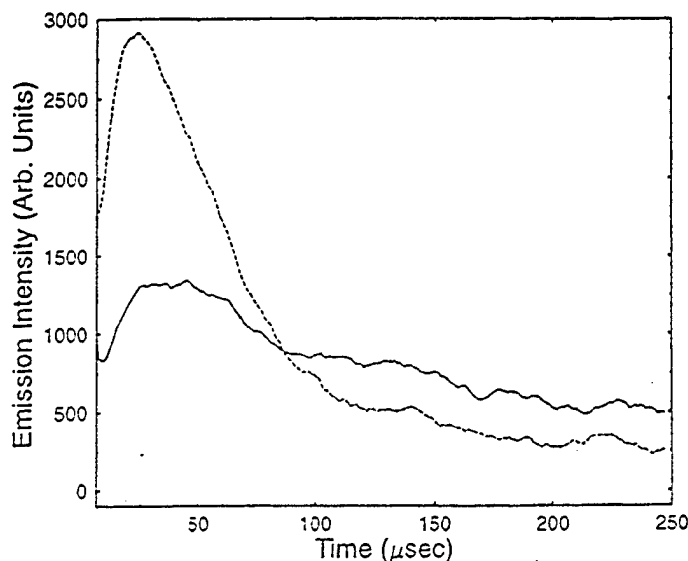


Figure 7. Time profiles of emission from  $\text{NF}(a)$  (broken line) and  $\text{NCl}(a)$  (solid line) produced by reaction of  $\text{NH}(a)$  with  $\text{ClF}$ .

## SYNTHESIS OF GROUP III AZIDES AND DEPOSITION OF III-V THIN FILMS

### 1. Gas Phase Synthesis, Structure, and Dissociation of Boron Triazide

This project began serendipitously, from experiments which were originally intended to probe the insertion of  $\text{NH}(a^1\Delta)$  into  $\text{BCl}_3$ . A spontaneous, room temperature reaction was observed upon mixing  $\text{HN}_3$  with gaseous  $\text{BCl}_3$ . The reaction was monitored by infrared spectroscopy, which showed that the  $\text{BCl}_3$  was completely removed by the addition of excess  $\text{HN}_3$ . Further, the  $\text{HN}_3$  was also removed and, for a carefully measured three-fold excess of the azide over  $\text{BCl}_3$ , the IR spectrum shown in Figure 8 was obtained. Careful measurements with many reaction mixtures verified the 3:1 stoichiometry associated with this species. From the simplicity of the spectrum, we thought that this species might be a symmetrical ( $\text{C}_3$ ) boron

triazide,  $B(N_3)_3$ . Such a molecule might be produced by successive addition of  $HN_3$  to  $BCl_3$  (via donation of the lone pair electrons on the  $N_3$  chain to the unoccupied p orbital on the boron atom), followed by elimination of  $HCl$ . Indeed, the  $HCl$  co-product is also evident in the spectrum of Figure 8. Boron triazide was prepared in 1954 by Wiberg and Michaud,<sup>20</sup> using low temperature condensed phase methods. Although a number of investigations<sup>21</sup> of azides of boron have been reported since that time, none were done in the gas phase and no spectra of  $B(N_3)_3$  have been noted.

To further investigate the possible generation of  $B(N_3)_3$  in the  $HN_3/BCl_3$  reaction, we performed a number of ab initio computations of the geometry and IR frequencies of this molecule. The calculations were done using the GAUSSIAN 92 family of programs<sup>22</sup> at both the Hartree - Fock and MP2 levels of theory, with a number of basis sets. Table III shows the results of the geometry optimization at the MP2/6-31G(d) level of theory, and Figure 9 shows

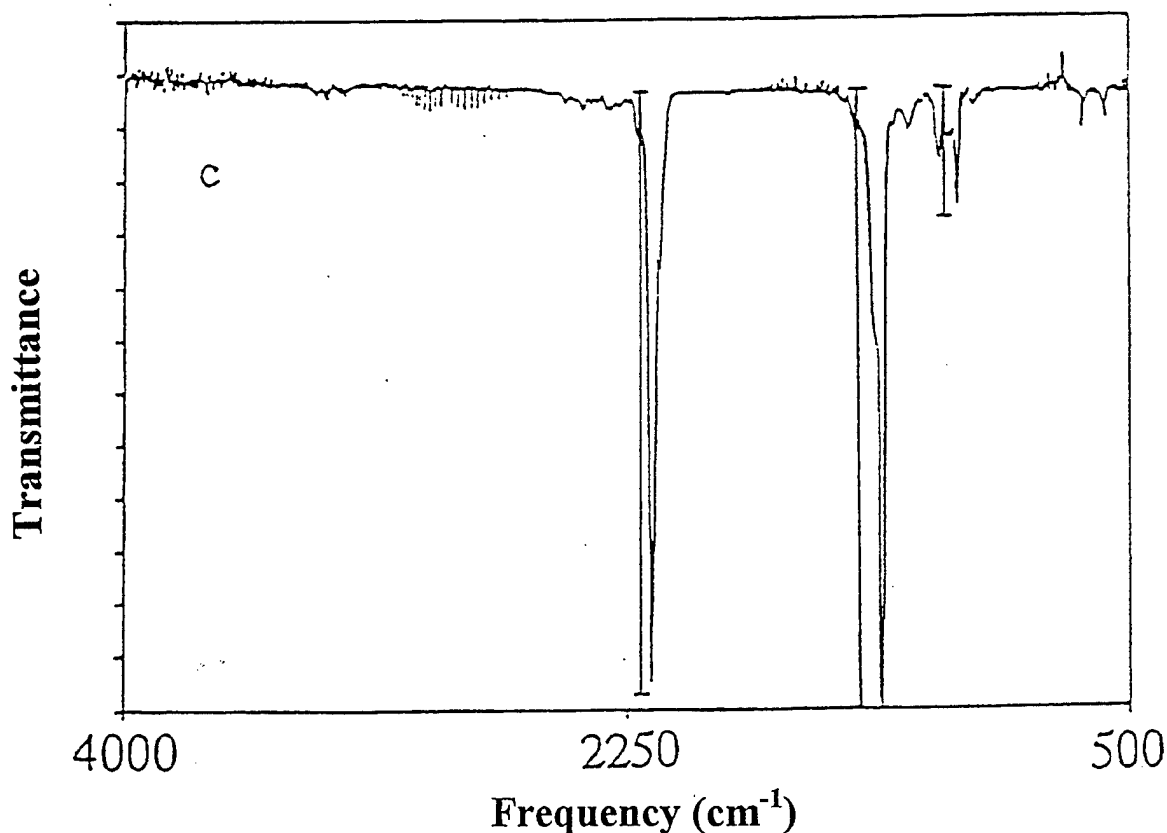


Figure 8. IR spectrum of the products of the reaction between gaseous  $BCl_3$  (0.3 Torr) and gaseous  $HN_3$  (0.9 Torr). Vertical bars indicate the results of an MP2/6-31G(d) calculation of the infrared frequencies of  $B(N_3)_3$ .

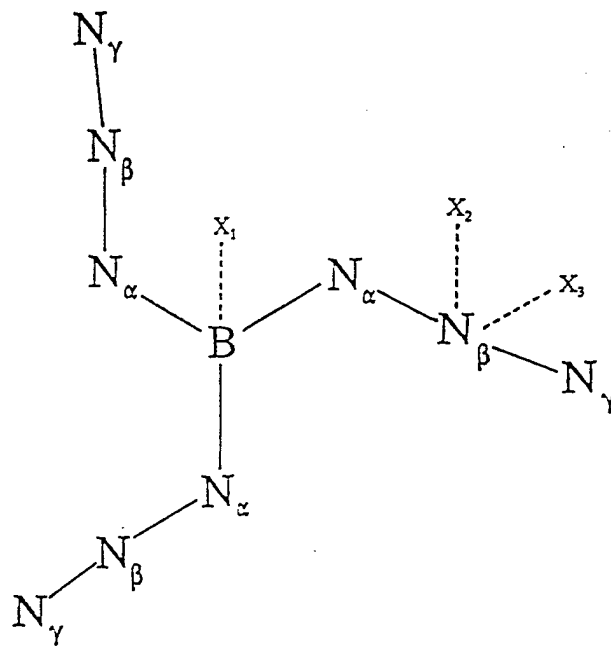


Figure 9. Calculated geometry of  $B(N_3)_3$  showing the variables of the calculation.

Table III. Calculated Geometries for  $B(N_3)_3$

Parameter <sup>a</sup>	HF/6-31G(d)	HF/6-31+ G(d)	MP2/6-31G(d)
B-N	1.440	1.439	1.442
$N_a-N_b$	1.240	1.241	1.241
$N_b-N_g$	1.092	1.092	1.166
$A_1 = \langle X_1-B-N_a \rangle$	90.0	90.2	90.2
$A_2 = \langle B-N_a-N_b \rangle$	117.5	117.7	120.4
$A_3 = \langle X_1-B-N_a-N_b \rangle$	90.0	90.0	90.0
$A_4 = \langle N_a-N_b-X_2 \rangle$	89.0	89.8	90.7
$= \langle X_2-N_b-X_3 \rangle$	89.0	89.8	90.7
$= \langle X_2-N_b-N_g \rangle$	89.0	89.8	90.7
$A_5 = \langle B-N_a-N_b-X_2 \rangle$	93.5	94.2	79.1
$A_6 = \langle N_a-N_b-X_3 \rangle$	87.4	87.4	86.5
$= \langle X_3-N_b-N_g \rangle$	87.4	87.4	86.5
$A_7 = \langle N_a-B-N_a \rangle$	120.0	120.0	120.0

<sup>a</sup>Parameters defined as in Figure 9. Distances in Angstroms, angles in degrees.

the corresponding structure. Table IV shows the results of frequency calculations at both the HF and MP2 levels, and the spectrum calculated at the MP2/6-31G(d) level is shown as a stick spectrum in Figure 8. Clearly, the agreement with the experimental spectrum is quite good, supporting our assignment of this spectrum to  $B(N_3)_3$ .

Table IV. Calculated Frequencies<sup>a</sup> for  $B(N_3)_3$

	$\nu_{17}/\nu_{18}$	$\nu_{21}/\nu_{22}$	$\nu_{23}/\nu_{24}$
HF/6-31G(d)	1209(134)	1435(1556)	2583(1094)
HF/6-31+G(d)	1202(144)	1426(1583)	2575(1152)
MP2/6-31G(d)	1146(181)	1451(862)	2202(841)

<sup>a</sup>Frequencies in  $\text{cm}^{-1}$ , relative intensities in parentheses

The geometry optimizations indicated that the heat of formation of the boron triazide molecule is about 21.2 kcal/mole, a value quite similar to that<sup>23</sup> of  $BH_3$ . The molecule is stabilized by the strength of its B-N bonds, at an average of 108 kcal/mole per bond. Nonetheless, dissociation to BN(solid) and four  $N_2$  molecules is exothermic by 81 kcal/mole, suggesting that this species could be a useful precursor for boron nitride thin films. This possibility was explored by investigations of the dissociation of the molecule by both thermal and photolytic means.

Samples of  $B(N_3)_3$  at densities near  $1 \times 10^{16} \text{ cm}^{-3}$  (in He diluent) were observed to decay spontaneously even at room temperature. Figure 10 shows the decay of one such sample measured (by IR and UV absorption) over more than an hour. The decay of the sample is nearly exponential, with a  $e^{-1}$  time constant near 30 minutes. Although no decay products were found in the IR absorption spectrum, a clearly visible whitish film formed on the cell walls and window during this time. This result, repeated many times, suggests that the boron triazide does indeed decompose to gaseous  $N_2$  and a boron-nitrogen film of some sort. Figure 11 shows an IR spectrum of the film, on a KCl substrate. The absorption features at 1263 and 720  $\text{cm}^{-1}$  are close to those expected<sup>24</sup> for hexagonal BN, but are shifted to the red, perhaps by the inclusion of excess nitrogen.

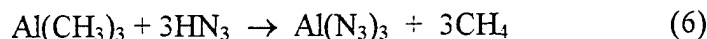
The UV-visible absorption spectrum of boron triazide was measured with a diode array spectrometer and the results are shown in Figure 12. A single large feature is evident near 230 nm, with an intensity corresponding to a cross section  $\sigma = 1.3 \times 10^{-17} \text{ cm}^2$ . Based on this information, a number of experiments were performed in which samples of  $B(N_3)_3$  were photolyzed with a 50 W xenon lamp, with the goal of depositing thin films on substrates positioned inside the photolysis chamber. Whitish films were easily produced, and an IR spectrum of such a film (on a MgF substrate) is shown in Figure 13. Although the 1263  $\text{cm}^{-1}$  feature observed from thermal dissociation is present, stronger features are evident at 1400 and 1100  $\text{cm}^{-1}$ , very close to the known frequencies<sup>24</sup> of hexagonal and cubic BN, respectively (shown by arrows in the figure).

A paper describing our experiments with the  $B(N_3)_3$  system was published<sup>25</sup> in the Journal of Physical Chemistry in 1995. The results clearly show the promise of this chemistry for the generation of boron nitride thin films. We are presently conducting experiments with a higher

vacuum apparatus and higher purity reagents, and are exploring the use of continuous flow deposition with careful control of reagent mixing ratios in an effort to generate higher quality BN films.

## 2. Aluminum Azides and AlN Thin Films

Like their boron analogues, various aluminum azides have been synthesized by a number of researchers<sup>26</sup> over the past 40 years, using wet chemistry methods that are often complex, dangerous, and clearly not suited to the high purity environment required for the deposition of thin films. Our objective was to explore the use of gas phase, room temperature HN<sub>3</sub> chemistry for the production of these species. Since AlCl<sub>3</sub> is non-volatile, a reaction analogous to the BCl<sub>3</sub> + HN<sub>3</sub> system used previously was not viable. Hence, we tried a reaction between Al(CH<sub>3</sub>)<sub>3</sub> and HN<sub>3</sub>, as follows:



This reaction should proceed by successive additions of HN<sub>3</sub> to the unoccupied p type orbital on the aluminum, followed by elimination of methane. Partially azidified methyl aluminum molecules are expected to be short-lived intermediates, when an appropriate excess of HN<sub>3</sub> is present.

The reagent gases were handled using a stainless steel vacuum line evacuated by a mechanical pump. A 10% mixture of HN<sub>3</sub> in He was prepared as described previously.<sup>27</sup> Trimethylaluminum (Alfa) was purified by freeze - thaw cycles at 273K to remove excess methane. The purities of both reagents were monitored by measurements of IR and UV absorption spectra. The reagents were mixed in a 10 cm sample cell equipped with KCl or KBr windows for IR transmission. The loss of the reagents in the cell and the formation of products was monitored by FTIR analysis of the gaseous contents. Figure 14 shows the behavior of the reagents, for various initial HN<sub>3</sub>/Al(CH<sub>3</sub>)<sub>3</sub> ratios. The data shown reflect absorbance measurements made 10 minutes after mixing. The Al(CH<sub>3</sub>)<sub>3</sub> concentration declines monotonically, reaching zero at HN<sub>3</sub>/Al(CH<sub>3</sub>)<sub>3</sub> = 3. This is also the point at which unreacted HN<sub>3</sub> reappears in the mixture. These results offer very strong evidence that the stoichiometry of the reaction is as shown in Eqn. 6 above, and that the reaction is proceeding to a fully azidified aluminum compound.

The spectra of the reaction mixtures also showed the appearance of reaction products. Though obscured by reagent absorptions, IR peaks near 741, 1236, and 2156 cm<sup>-1</sup> were correlated with products. In an effort to more clearly identify the aluminum azide products, a number of experiments were performed using low temperature matrix isolation methods. In these experiments, continuously flowing streams of Al(CH<sub>3</sub>)<sub>3</sub> and HN<sub>3</sub> in the 1:3 ratio were allowed to react in a glass vessel and then passed over a cold window held at 10K. The residence time of the gasses in the glass vessel was set near 10 minutes in order to ensure complete reaction. These experiments were very successful in the sense that the features attributable to aluminum azides were much better resolved, as expected at this low temperature. The results are shown along with the room temperature data in Table V.

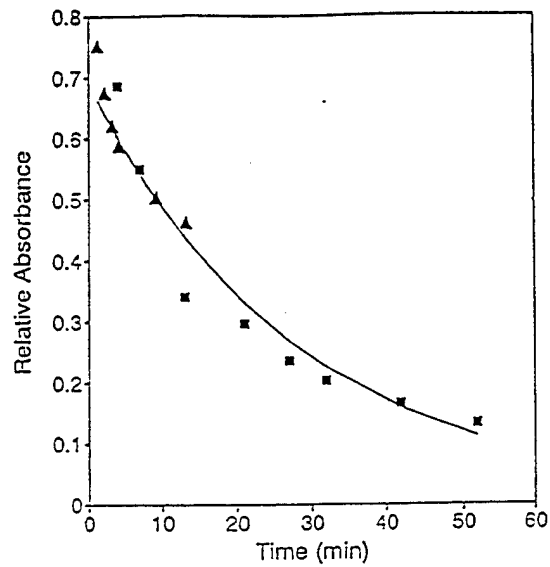


Figure 10. Time decay of a sample of 0.3 Torr of  $B(N_3)_3$ .

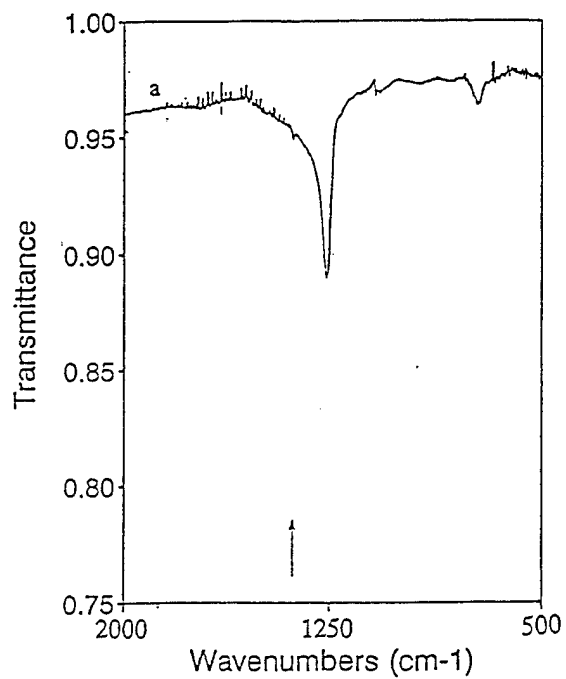


Figure 11. Infrared spectra of films deposited by the athermal dissociation of  $B(N_3)_3$ . Arrows indicated frequencies ascribed to hexagonal BN.

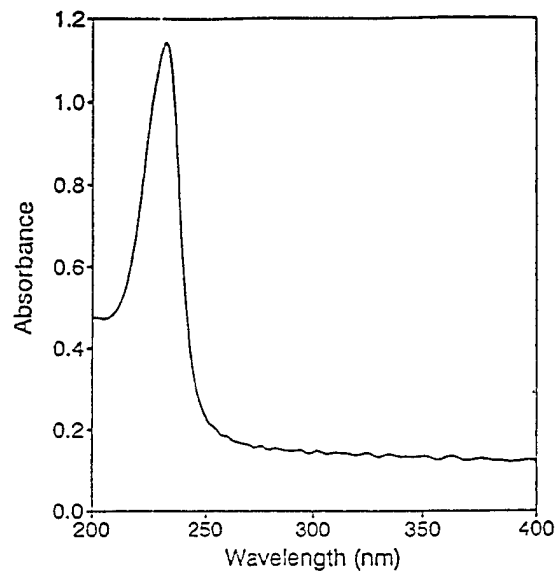


Figure 12. Ultraviolet absorption spectrum of  $B(N_3)_3$  at a pressure of 0.3 Torr.

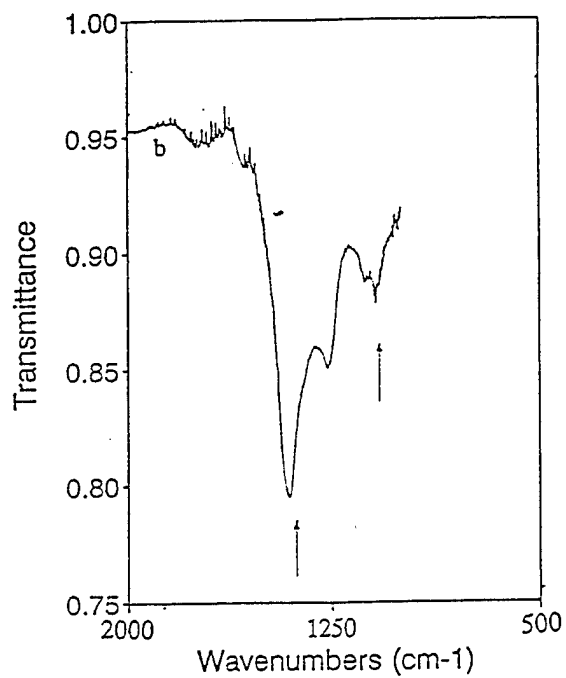


Figure 13. IR spectrum of film produced by photodissociation of  $B(N_3)_3$ . Arrows indicate frequencies of hexagonal and cubic BN.

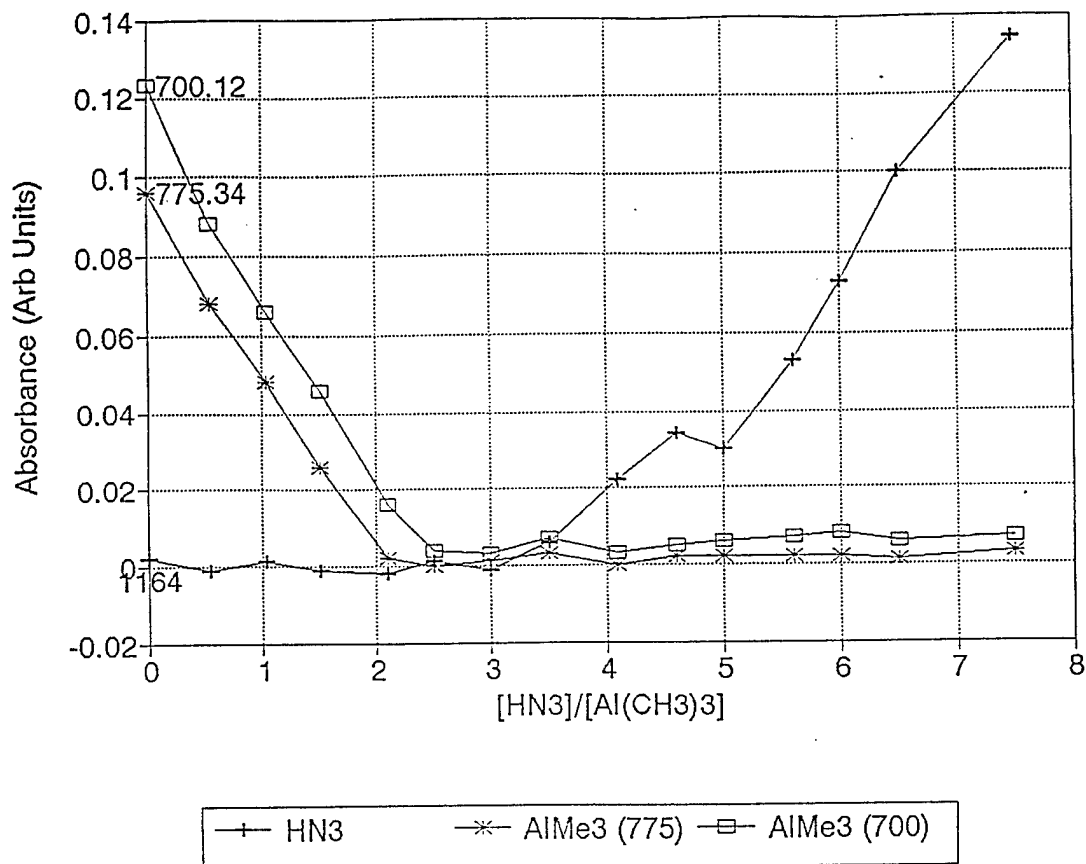


Figure 14. Plot of the IR absorbances of  $\text{HN}_3$  and  $\text{Al}(\text{CH}_3)_3$  at various reaction stoichiometries.

In order to ascertain whether such features would correspond to the desired  $\text{Al}(\text{N}_3)_3$  molecule, a series of ab initio calculations were performed in order to determine the structure and IR frequencies expected for this species. The calculations were performed using the GAUSSIAN 92 family of programs<sup>22</sup>, and employed a number of basis sets at both the RHF and MP2 levels of theory. Table VI shows the results of geometry optimizations which used a 6-31G(d) basis set. The data indicate that, like  $\text{B}(\text{N}_3)_3$ , the  $\text{Al}(\text{N}_3)_3$  molecule is a nearly planar pinwheel structure. The major difference from the boron compound is the  $\text{Al-N}_\alpha\text{-N}_\beta$  angle, which is nearly ten degrees greater in the aluminum compound and indicates substantially more "s" character in the occupied orbitals of  $\text{N}_\alpha$ . Frequency calculations were performed at the MP2/6-31G(d) level for the optimized geometry, and the results are shown in Table V, along with the comparable data from the experiments noted above. The results are in very good agreement with the frequencies found in the gas phase and low temperature matrix IR spectra of the reaction products, and, taken with the stoichiometry data described above, offer strong evidence that the reaction proceeds to completion with the formation of  $\text{Al}(\text{N}_3)_3$ .

After several reaction mixtures had been allowed to react in the cell, IR features were observed to grow in in the background spectrum of the cell, indicating the formation of a film on the cell windows. Figure 15 shows the IR spectrum of such a film. The low frequency absorptions in the  $600\text{-}900\text{ cm}^{-1}$  region clearly correspond to well known<sup>28</sup> phonon modes in  $\text{AlN}$ . The spectrum also shows a pair of high frequency features, at

**Table V: Calculated Frequencies for Al(N<sub>3</sub>)<sub>3</sub>**

Level of Theory	$\nu$ (AlNNN) (Rel. Intensity)	$\delta$ (N <sub>3</sub> ) (Rel. Intensity)	$\nu$ sym. (N <sub>3</sub> ) (Rel. Intensity)	$\nu$ assym. (N <sub>3</sub> ) (Rel. Intensity)
RMP / 6-31 G(d)	568 cm <sup>-1</sup> (21)	737 cm <sup>-1</sup> (251)	1366 cm <sup>-1</sup> (210)	2192 cm <sup>-1</sup> (1011)
Observed : Gas Phase	-----	741 cm <sup>-1</sup>	1236 cm <sup>-1</sup>	2156 cm <sup>-1</sup>
Observed : Matrix Studies	-----	730 cm <sup>-1</sup>	1360 cm <sup>-1</sup>	2160 cm <sup>-1</sup>

**Table VI: Calculated Geometry Parameters for Al(N<sub>3</sub>)<sub>3</sub>**

Parameter	RHF / 6-31 G(d)	RMP2 / 6-31 G(d)
Al-N <sub>α</sub> (Å)	1.768	1.787
N <sub>α</sub> -N <sub>β</sub> (Å)	1.215	1.229
N <sub>β</sub> -N <sub>γ</sub> (Å)	1.099	1.175
∠ X <sub>1</sub> * - Al - N <sub>α</sub> (degrees)	90.0	90.0
∠ Al - N <sub>α</sub> - N <sub>β</sub> (degrees)	134.1	133.4
∠ X <sub>1</sub> * - Al - N <sub>α</sub> - N <sub>β</sub> (degrees)	90.1	90.1
∠ X <sub>2</sub> ** - N <sub>β</sub> - N <sub>α</sub> (degrees)	90.1	90.3
∠ Al - N <sub>α</sub> - N <sub>β</sub> - X <sub>2</sub> ** (degrees)	86.7	84.4
∠ X <sub>3</sub> ** - N <sub>β</sub> - N <sub>α</sub> (degrees)	88.2	87.4
∠ N <sub>α</sub> - Al - N <sub>α</sub> (degrees)	120	120

\* X<sub>1</sub>: Dummy atom placed on Al

\*\* X<sub>2</sub>, X<sub>3</sub>: Dummy atoms placed on N<sub>β</sub>.

2043 cm<sup>-1</sup> and 2111 cm<sup>-1</sup>. These are identified as corresponding to Al(N<sub>3</sub>)<sub>3</sub> condensed in the film (indeed, the fully azidified aluminum is expected to be condensed) and to the Al-N<sub>2</sub> complex, respectively. The Al-N<sub>2</sub> complex has been observed by Mazur and Cleary<sup>29</sup> in the preparation of AlN films, at IR frequencies corresponding closely with those found in our experiments. Upon gentle heating of the substrate and film to roughly 325K, the 2043 cm<sup>-1</sup> peak was found to be diminished and the 2111 cm<sup>-1</sup> peak grew in intensity. We attribute this result to thermal dissociation of the Al(N<sub>3</sub>)<sub>3</sub> present in the film to form the Al-N<sub>2</sub> complex. When the film was heated to 400K for a period of 1 hour, the Al(N<sub>3</sub>)<sub>3</sub> and Al-N<sub>2</sub> features were lost entirely. Figure 16 shows an IR spectrum of this result, along with a spectrum of an AlN film produced by laser ablation of an AlN target<sup>30</sup>. The

agreement is excellent, and indicates that the heating removed all excess nitrogen from our film, leaving only AlN. This result offers an interesting low temperature route to AlN thin films, which we intend to investigate further using reagents of higher purity and a higher vacuum apparatus. The results obtained to date were assembled into a manuscript<sup>31</sup> which was recently accepted for publication in the Journal of Physical Chemistry.

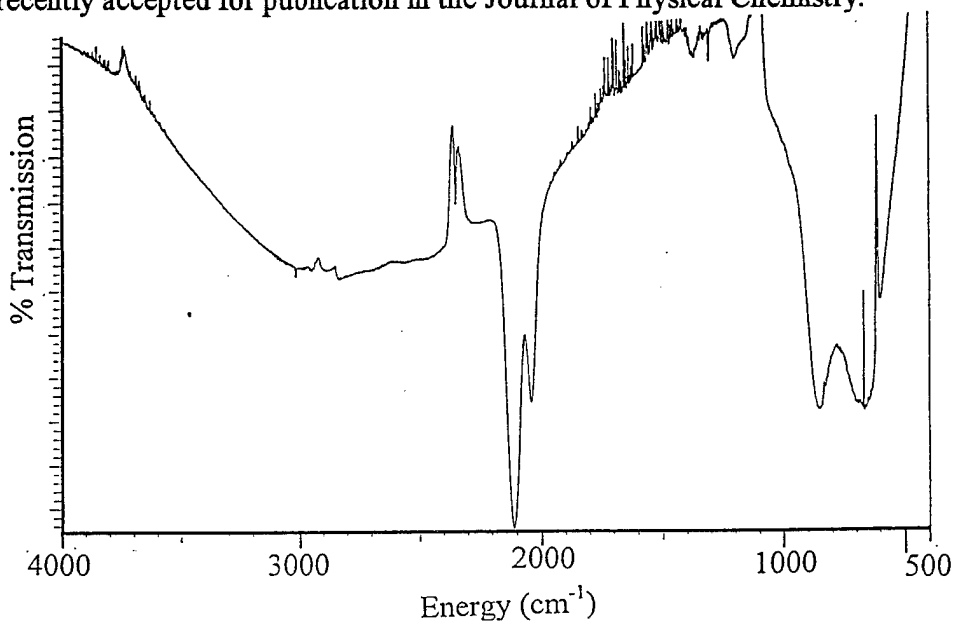


Figure 15. IR spectrum of film produced by reaction of  $\text{HN}_3$  with  $\text{Al}(\text{CH}_3)_3$  at a 3:1 mixing ratio

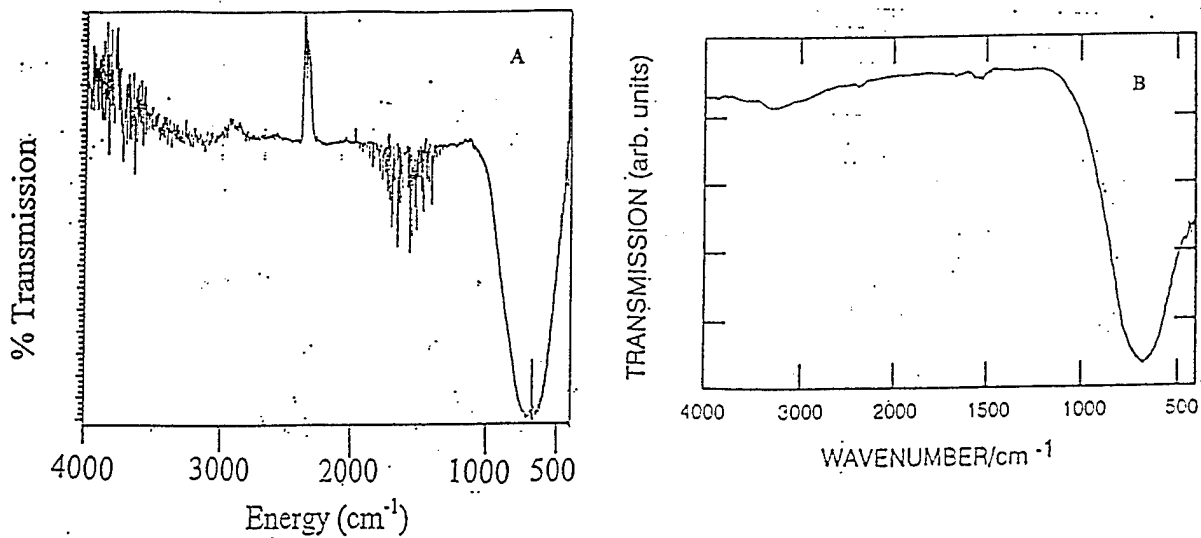


Figure 16. (a) Film as in Figure 15 after exposure to 400K for 60 minutes.  
(b) IR spectrum of AlN film produced by laser ablation (ref. 30).

### 3. The Reaction of Ga(CH<sub>3</sub>)<sub>3</sub> with HN<sub>3</sub>

A number of researchers have attempted to use azides for the low temperature generation of GaN thin films. GaN films have drawn intense interest since this material has a bandgap corresponding to the emission of blue-green radiation, and GaN diodes have been recently demonstrated<sup>32</sup>. Kouvetakis and co-workers<sup>33</sup> have used wet-chemistry methods to produce gallium azides, which were then thermally decomposed at high temperatures to generate GaN. Lin and co-workers<sup>34,35</sup> have used traditional CVD methods to produce films GaN and InN from high temperature reactions between metal organics of the group III metals and HN<sub>3</sub>. We have recently begun working on the reaction of Ga(CH<sub>3</sub>)<sub>3</sub> with HN<sub>3</sub>, in the hope of generating GaN thin films from mechanisms such as those operative in our work on BN and AlN. Tables VII and VIII show the results of ab initio calculations of the geometry and frequencies, respectively, of Ga(N<sub>3</sub>)<sub>3</sub> done at the MP2/LANL2DZ level of theory. It is interesting to note that the Ga-N<sub>α</sub>-N<sub>β</sub> bond angle is much larger than the analogous angle in Al(N<sub>3</sub>)<sub>3</sub>, and that the N<sub>α</sub>-N<sub>β</sub> bond length is not much larger than the N<sub>β</sub>-N<sub>γ</sub> bond length. Both results suggest that Ga(N<sub>3</sub>)<sub>3</sub> is a much more ionic compound than Al(N<sub>3</sub>)<sub>3</sub> or B(N<sub>3</sub>)<sub>3</sub>, with possible significant effects on the decomposition mechanism. The results of our initial experiments with this system have been very encouraging. Figure 17 shows the IR spectrum of a thin film produced by reacting Ga(CH<sub>3</sub>)<sub>3</sub> with HN<sub>3</sub> at a 1:3 stoichiometry at room temperature, followed by evacuation to remove the residual gases over the film. As with the AlN studies above, the film is expected to contain non-volatile Ga(N<sub>3</sub>)<sub>3</sub> as well as any GaN and complexed N<sub>2</sub> formed by its decomposition. The features at 2110 cm<sup>-1</sup> and 1251 cm<sup>-1</sup> are in good agreement with the results of the MP2/LANL2PZ calculation shown in Table VIII. These are very preliminary results, and we have not yet attempted to heat the film to produce GaN (by analogy with the AlN chemistry described above). Nonetheless, our approach seems to hold great promise.

Table VII. Calculated Geometry Parameters for Ga(N<sub>3</sub>)<sub>3</sub>

Parameter	RHF / Lanl2dz	MP2 / Lanl2dz
Ga-N <sub>α</sub> (Å)	1.768	1.804
N <sub>α</sub> -N <sub>β</sub> (Å)	1.224	1.254
N <sub>β</sub> -N <sub>γ</sub> (Å)	1.124	1.233
∠ Al - N <sub>α</sub> - N <sub>β</sub> (degrees)	148.1	145.8
∠ N <sub>α</sub> - N <sub>β</sub> - N <sub>γ</sub> (degrees)	176.2	173.6
∠ N <sub>α</sub> - Al - N <sub>α</sub> (degrees)	120.0	120.0
∠ X <sub>2</sub> - N <sub>β</sub> - N <sub>α</sub> (degrees)	90.1	90.3
∠ N <sub>β</sub> - N <sub>α</sub> - Al - N <sub>α</sub> (degrees)	0.03	0.05

**Table VIII. Calculated Frequencies for Ga(N<sub>3</sub>)<sub>3</sub>**

Level of Theory	$\nu_{11}^{**}, \nu_{12}^{**}$ (Rel. Intensity)	$\nu_{13}^{**}, \nu_{14}^{**}, \nu_{15}^{**}$ (Rel. Intensity)	$\nu_{19}^{**}, \nu_{20}^{**}$ (Rel. Intensity)	$\nu_{22}^{**}, \nu_{23}^{**}, \nu_{24}^{**}$ (Rel. Intensity)
RHF / LANL2DZ	473 cm <sup>-1</sup> (141)	614 cm <sup>-1</sup> (554)	1343 cm <sup>-1</sup> (865)	2117 cm <sup>-1</sup> (2047)
MP2 / LANL2DZ	449 cm <sup>-1</sup> (5)	468 cm <sup>-1</sup> (72)	1222 cm <sup>-1</sup> (131)	2065 cm <sup>-1</sup> (835)

\* MP2 modes

\* RHF modes

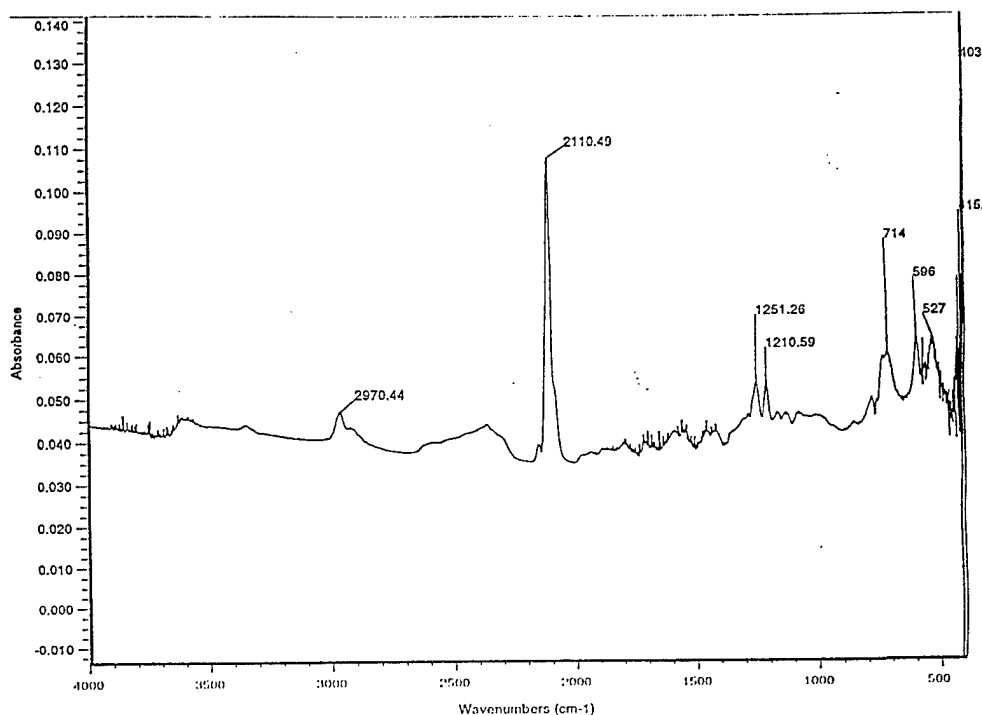


Figure 17. IR spectrum of a film produced by reaction of HN<sub>3</sub> with Ga(CH<sub>3</sub>)<sub>3</sub> at a 3:1 mixing ratio.

## CONCLUSIONS AND FUTURE WORK

The research performed in the course of this AFOSR - sponsored program has produced a number of significant results. The NILE laser device is the first new electronic transition chemical laser in many years, and comes at a time when the Air Force is actively seeking alternatives to the two phase chemistry used to power the high energy COIL laser devices. While still in a fledgling stage of development, the NILE offers the possibility of an all gas phase system, with several different chemical systems potentially usable for the chemical generation of the excited NCl(a) energy carrier. A particularly pleasing point about the NILE system investigated in our lab has been that the energy which powers the device is chemical energy stored in ClN<sub>3</sub> and released by the chain decomposition of this energetic nitrogen compound. This offers us many possible ways to initiate and sustain the laser chemistry. One of the most interesting of these is dissociation of the ClN<sub>3</sub> by collisions with vibrationally excited N<sub>2</sub>. One can envision a NILE device much like a high energy CO<sub>2</sub> laser, in which the inversion is pumped by energy transfer from N<sub>2</sub>(v) generated in an electric discharge or gas dynamic expansion. We are presently

investigating the details of energy exchange between vibrationally excited  $N_2$  and  $CIN_3$ , using both discharge flow and pulsed laser (real time) methods. Further, we are performing experiments in which we are exciting iodine atoms by electric discharge through  $CIN_3$ /diluent/ $I_2$  mixtures in a 2 m long  $CO_2$  laser head (A Lumonics 103 laser). Initial results have shown that this system behaves very much like the excimer laser photolysis system used for the original NILE tests, but is hampered by  $I^*$  quenching by the undissociated  $I_2$  in the cavity. We are currently searching for alternate sources of iodine atoms for this system.

The projects involving the synthesis and dissociation of group III azides have been very exciting and interesting since this entire area of research is virtually unknown territory, with very little in the literature to lead us on our way. The results we have produced clearly offer the possibility of very low temperature deposition of group III nitrides, which are extremely important electronic materials. In order to realize this potential, we need to forge ties with those in the traditional electronic materials community. Making such links between different disciplines (our work to date is largely chemistry, and must somehow be translated into the electrical engineering and materials science world) can be difficult. We have begun by establishing a collaboration with Professor George Collins at Colorado State University, an electrical engineer whose work on thin film deposition and etching is well known. As noted above, we are currently working on the GaN system, and preliminary results obtained as a part of a new AFOSR program (F49620-97-1-0036) have been most encouraging. In addition, we are continuing our research with the  $B(N_3)_3$  and  $Al(N_3)_3$  systems. Dissociation of these azides by photolysis or thermolysis can produce a number of very interesting radical species which may be important in several BN and AlN deposition methods. We are collaborating with Professor Juliana Gilbert of the Chemistry and Biochemistry Department at DU in an effort to trap these radicals in low temperature matrices. The initial experiments have been very successful. Finally, in a flight of fancy, we have begun an investigation of the possible existence of  $N(N_3)_3$  ! Preliminary calculations have suggested that this molecule is indeed stable.

#### PUBLICATIONS ARISING FROM THIS WORK

1. A.J. Ray and R.D. Coombe, "Collisional Quenching of  $NCl(a^1\Delta, v=0)$  and the Chain Decomposition of  $CIN_3$ ", *J. Phys. Chem.*, **98**, 8940, (1994).
2. R.L. Mulinax, G.S. Okin, and R.D. Coombe, "Gas Phase Synthesis, Structure, and Decomposition of Boron Triazide", *J. Phys. Chem.*, **99**, 6294 (1995).
3. A.J. Ray and R.D. Coombe, "An  $I^*$  Laser based on Energy Transfer from  $NCl(a^1\Delta)$ ", *J. Phys. Chem.*, **99**, 7849 (1995).
4. S.M. Singleton and R.D. Coombe, "Quenching of  $NH(a^1\Delta)$  by Molecular Halogens and Interhalogens", *J. Phys. Chem.*, **99**, 16296 (1995).

5. C.J. Linnen, D.E. Macks, and R.D. Coombe, "Synthesis of  $\text{Al}(\text{N}_3)_3$  and the Deposition of AlN Thin Films", *J. Phys. Chem.*, in press (1997).

6. A.J. Ray Hunter and R.D. Coombe, "Efficient Production of  $\text{NCl}(a^1\Delta)$  by the F/Cl +  $\text{HN}_3$  System and Energy Transfer to Iodine Atoms", manuscript in preparation for submission to *J. Phys. Chem.*

In addition, we expect our preliminary studies of the  $\text{Ga}(\text{CH}_3)_3 + \text{HN}_3$  system to be completed shortly, and a paper describing this work (supported by both this AFOSR grant and the new grant, F49620-97-1-0036) will be prepared.

### PERSONNEL

Principal Investigator: Dr. Robert D. Coombe

Graduate Research Associates:

Stephen M. Singleton (Ph.D. 1995)

Amy J. Ray (Ph.D. 1996)

Christopher J. Linnen (M.S. 1996)

Undergraduate Research Associates

Rhonda L. Mulinax

Gregory S. Okin

Daniel E. Macks

### REFERENCES

1. R.D. Coombe, D. Patel, A.T. Pritt, Jr., and F.J. Wodarczyk, *J. Chem. Phys.* *75*, 2177 (1981); R.D. Coombe and M.H. Van Benthem, *J. Chem. Phys.*, *81*, 2984(1984).

2. D.J. Benard, M.A. Chowdhury, B.K. Winkler, T.A. Seder, and H.H. Michels, *J. Phys. Chem.*, *94*, 8507 (1990).

3. A.J. Ray and R.D. Coombe, *J. Phys. Chem.*, *98*, 8940 (1994).

4. A.J. Ray and R.D. Coombe, *J. Phys. Chem.*, *97*, 3475 (1993).

5. R.D. Bower and T.T. Yang, *J. Opt. Soc. Amer.*, *B8*, 1583 (1991).

6. E. Gerck, *J. Chem. Phys.*, *79*, 311 (1983).

7. W.H. Pence, S.L. Baughcum, and S.R. Leone, *J. Chem. Phys.*, *85*, 3844 (1981).

8. P.J. Dyne and D.W.G. Style, *J. Chem. Soc.*, 2122 (1952); D.W.G. Style and J.C. Ward, *J. Chem. Soc.*, 2125 (1952).
9. W.G. Brown, *Phys. Rev.*, *38*, 1187 (1931).
10. A.J. Ray and R.D. Coombe, *J. Phys. Chem.*, *99*, 7849 (1995).
11. D.R. Yarkony, *J. Chem. Phys.*, *86*, 1642 (1987).
12. G.R. Bradburn and H.V. Lilenfeld, *J. Phys. Chem.*, *95*, 555 (1991).
13. J. Habdas, S. Wategaonkar, and D.W. Setser, *J. Phys. Chem.*, *91*, 451 (1987).
14. D.J. Benard, private communication, 1996.
15. D.B. Exton, J.V. Gilbert, and R.D. Coombe, *J. Phys. Chem.*, *95*, 2692 (1991).
16. S.M. Singleton and R.D. Coombe, *Chem. Phys. Lett.*, *215*, 237 (1993).
17. D.B. Exton, J.V. Gilbert, and R.D. Coombe, *J. Phys. Chem.*, *95*, 7758 (1991).
18. E. Arunan, C.P. Liu, D.W. Setser, J.V. Gilbert, and R.D. Coombe, *J. Phys. Chem.*, *98*, 494 (1994).
19. S.M. Singleton and R.D. Coombe, *J. Phys. Chem.*, *99*, 16296 (1995).
20. E. Wiberg and H. Michaud, *Z. Naturforsch.*, *96*, 497 (1954).
21. See for example P.O. Paetzold *Z. Anorg. Allg. Chem.*, *326*, 47, 53, 58, 64 (1963).
22. J.M. Frisch, G.W. Trucks, M. Head-Gordon, P.M. Gill, M.W. Wong, J.B. Foresman, B.G. Johnson, H.B. Schlegel, M.A. Robb, E.S. Repogle, R. Gomperts, J.L. Andres, K. Raghavachari, J.S. Binkley, C. Gonzales, R.L. Martin, D.J. Fox, D.J. DeFrees, J. Baker, J.J. Sttewart, and J.A. Pople, GAUSSIAN 92, Gaussian, Inc. Pittsburgh, PA, 1992.
23. M.W. Chase, C.A. Davies, J.R. Downey, D.J. Frurip, R.A. McDonald, and A.N. Sverud, JANAF Thermochemical Tables, 3rd Ed., *J. Phys. Chem. Ref. Data*, *14* (1985).
24. V. Cholet, L. Vandenbulke, and J.P. Rouan, *J. Mat. Sci.*, *29*, 6 (1994); R. Ishihara, O. Sigiura, and M. Matsumura, *Appl. Phys. Lett.*, *60*, 3244 (1992).
25. R.L. Mulinax, G.S. Okin, and R.D. Coombe, *J. Phys. Chem.*, *99*, 6294 (1995).
26. See for example D.C. Boyd, R.T. Hasch, D.R. Mantell, R.K. Schulze, J.F. Evans, and W.L. Gladfelter, *Chem. Mater.*, *1*, 119 (1989).

27. See for example S.J. David and R.D. Coombe, *J. Phys. Chem.*, *89*, 5206 (1985).
28. A.T. Collins, E.C. Lightowers, and P. Dean, *Phys. Rev.* *158*, 3, 833 (1967).
29. U. Mazur and A.C. Cleary, *J. Phys. Chem.*, *94*, 189 (1990); X.D. Wang, K.W. Hipps, and U. Mazur, *J. Chem. Phys.*, *96*, 8485 (1992).
30. K. Seki, X. Xu, H. Okabe, J. Frye, and J. Halpern, *Appl. Phys. Lett.*, *60*, 2234 (1992).
31. C.J. Linnen, D.E. Macks, and R.D. Coombe, *J. Phys. Chem.*, in press (1997).
32. S. Nakamura, M. Senoh, S. Nagahama, N. Iwasa, T. Yamada, T. Matsushita, H. Kiyoku, and Y. Sugimoto, *Jpn. J. Appl. Phys.*, *35*, L217 (1996).
33. J. Kouvetakis and D.B. Beach, *Chem. Mater.*, *1*, 476 (1989).
34. Y. Bu, L. Ma, and M.C. Lin, *J. Vac. Sci. Technol. A*, *11*, 2931 (1993).
35. Y. Bu, M.C. Lin, L.P. Fu, D.G. Ctchekine, G.D. Gilliland, Y. Chen, S.E. Ralph, and S.R. Stock, *Appl. Phys. Lett.*, *66*, 2433 (1995).